Proton and α-radioactivity of spherical proton emitters

M. Balasubramaniam and N. Arunachalam
Department of Physics, Manonmaniam Sundaranar University, Tirunelveli-627012, India
(Received 1 September 2004; published 12 January 2005)

The half-lives of different spherical proton emitters are calculated. The preformed cluster model modified into a unified fission model of Gupta and collaborators with the effects of Coulomb repulsion, nuclear attraction due to proximity potential, and rotational energy due to angular momentum is used for the calculations. This includes the study of observed ground and isomeric state proton emitters of 26 proton-rich nuclei. The results are compared with experimental results and other theoretical calculations. The calculated results are in fair agreement with experimental values. It is evident from some experiments that α decay is a competing mode of branching for proton decay. Hence, the half-lives of α decay from these proton emitters are also presented for s waves.

DOI: 10.1103/PhysRevC.71.014603 PACS number(s): 23.50.+z, 21.10.Tg, 21.60.Gx, 23.60.+e

I. INTRODUCTION

The nuclei lying above the proton drip line with $Q_p > 0$ are proton unstable. These nuclei are very neutron deficient (i.e., proton rich). The phenomenon of proton emission from the nuclear ground states limits the possibilities of creation of ever more exotic nuclei in the proton-rich side of the β-stability valley. The process of proton decay is a nuclear reaction that can be written as

$$ {}^{A}_{Z}(X)_N \rightarrow {}^{A-1}_{Z-1}(Y)_N + {}^{1}_{1}(H) + Q_p, \tag{1} $$

where the Q_p value (in MeV) is positive for its spontaneous decay. Apart from providing information about the limits above the proton dripline, these studies can be used as a tool to obtain spectroscopic information because the decaying proton is the unpaired proton not filling its orbit, the decay rates of which are sensitive to the Q value and the orbital angular momentum, which in turn helps to determine the orbital angular momentum of the emitted proton. So far, proton radioactivity has been identified from the different isotopes of Sb, Tm, Lu, Ta, Re, Ir, Au, Tl, and Bi (spherical proton emitters) and from I, Cs, La, Eu, and Ho (deformed proton emitters) nuclei in their ground states (for some cases from the isomeric state) in two mass regions A $\sim$ 100 to 130 and A $\sim$ 140 to 180, corresponding to charges Z = 51–63 and Z = 67–80, respectively. Improved detection techniques, such as a double-sided silicon strip detector, made possible the discovery of several proton emitters having production cross sections as low as 100 μb, including the heaviest to date, ^{185}Bi [1]. Several theoretical attempts [2–4] were made to study this exotic process. The proton being considered as a point charge has the highest probability of being present in the parent nucleus and also has a low Coulomb potential and a high centrifugal barrier; hence this process can be dealt with within a simple WKB barrier penetration model. In the existing theoretical models [2,3], Woods-Saxon type potential is used for the nuclear part of the potential. In this work we have applied a unified fission model (UFM) modified from the preformed cluster model (PCM) of Gupta and collaborators [5,6], which has been successfully used in studies of cluster radioactivity. This model, which includes the effects of Coulomb repulsion, nuclear attraction due to proximity potential, and rotational energy due to angular momentum, is used for the first time to calculate proton emission from spherical proton emitters. Ground and isomeric proton as well as alpha decay branches are reported in some experiments [1,7] for the proton emitters ^{169}Ir, ^{173}Au, ^{177}Tl, and ^{185}Bi. Hence, using the same model, the α decay half-lives of all the proton emitters are studied for the s wave.

The model details are presented in Sec. II. In Sec. III the calculations and results of proton decay are presented. In Sec. IV the half-lives for α decay of the proton emitters are presented. In Sec. V the summary and conclusions of the present study are presented.

II. PREFORMED CLUSTER MODEL AS A UNIFIED FISSION MODEL

For our calculations we have used a unified fission model modified from the preformed cluster model of Gupta and collaborators [5,6]. The decay constant (and hence the half-life) in the PCM is defined as

$$ \lambda = \nu_0 P P_0 \tag{2} $$

$$ T_{1/2} = \ln 2/\lambda. \tag{3} $$

Here ν_0 is the impinging frequency with which the proton hits the barrier, P is the probability of penetrating the barrier, and P_0 is the preformation probability. To apply this model for proton decay it is assumed that the preformation probability $P_0 = 1$ for the emitted proton, and the tunneling is considered to start at the parent nucleus radius R_0 itself, instead of from the touching configuration as in the PCM (see Fig. 1). The WKB action integral for the penetration probability P as given below is solved numerically.

$$ P = \exp\left[-\frac{2}{\hbar}\int_{R_a}^{R_b}\{2\mu[V(R) - Q_p]\}^{1/2} dR\right], \tag{4} $$

with $V(R_a = R_0) = V(R_b) = Q_p$ value. R_a and R_b are respectively the first and second turning points. This means that the tunneling begins at $R = R_a(= R_0)$ and terminates at $R = R_b$, with $V(R_b) = Q_p$ value for ground state decay. The potential $V(R)$ is constituted of two parts in the overlapping

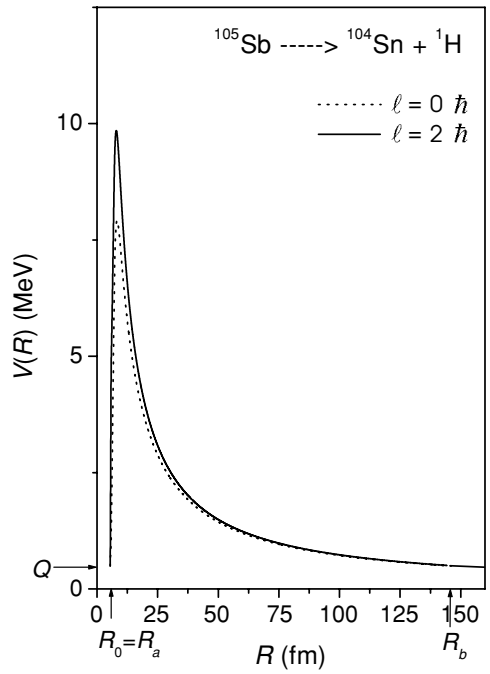

FIG. 1. The scattering potentials for the emission of a proton from ^{105}Sb at $\ell = 0\,\hbar$ (dotted line) and $\ell = 2\,\hbar$ (solid line) are plotted. The characteristic quantities (the turning points) R_a and R_b are shown. The decay Q value is also marked.

and nonoverlapping regions. For $R < C_t$ (overlapping region), $V(R)$ is parameterized simply as a polynomial of degree two in R and for $R \geqslant C_t$ (nonoverlapping region) the potential $V(R)$ is defined as the sum of the repulsive Coulomb potential, the attractive short range nuclear proximity potential (V_P) [8], and the centrifugal potential (V_ℓ) due to angular momentum. Here C_t is the touching configuration of two nuclei, with C_i as the Süsmann central radii

$$C_i = R_i - \frac{b^2}{R_i}, \tag{5}$$

where b is the surface width.

$$R_i = 1.28A_i^{1/3} - 0.76 + 0.8A_i^{-1/3}\ \text{fm}, \tag{6}$$

with $i = 1, 2$ corresponding to the daughter nucleus and the emitted proton. The fragments here are considered as spherical. Deformation effects are not taken into consideration in this work. The potential $V(R)$ is given as

$$V(R) = \begin{cases} a_1 R + a_2 R^2 & \text{for} \quad R_0 \leqslant R < C_t \\ \frac{Z_1 Z_2 e^2}{R} + V_p + V_\ell & \text{for} \quad R \geqslant C_t. \end{cases} \tag{7}$$

The constants a_i $(i = 1, 2)$ occurring in the polynomial are determined by using the following boundary conditions:

1. At $R = R_0 = R_a$, $V(R) = Q_p$.
2. At $R = C_t$, $V(R) = V(C_t)$.

The V_P is an additional attraction due to the nuclear proximity potential [8], which is given as

$$V_P = 4\pi \bar{R}\gamma b\Phi(s), \tag{8}$$

where $\bar{R}$ is the inverse of the root mean square radius of the Gaussian curvature. The specific nuclear surface tension γ is given by

$$\gamma = 0.9517\left[1 - 1.7826\left(\frac{N-Z}{A}\right)^2\right]\text{MeV fm}^{-2}. \tag{9}$$

The universal function $\Phi(s)$, which is independent of the geometry of the system, is given by

$$\Phi(s) = \begin{cases} -\frac{1}{2}(s-2.54)^2 - 0.0852(s-2.54)^3 \\ \quad \text{for} \quad s \leqslant 1.2511 \\ -3.437\exp\left(-\frac{s}{0.75}\right) \\ \quad \text{for} \quad s > 1.2511 \end{cases} \tag{10}$$

$$\bar{R} = \frac{C_1 C_2}{C_t}. \tag{11}$$

In Eq. (10), $s(=\frac{R-C_t}{b})$ is the overlap distance in units of b between the colliding surfaces. The surface width

$$b = 0.99\ \text{fm}. \tag{12}$$

Also, for the angular momentum effects,

$$V_\ell = \frac{\hbar^2 \ell(\ell+1)}{2I}. \tag{13}$$

In the nonsticking limit, the moment of inertia in Eq. (13) is given by

$$I = I_{\text{NS}} = \mu R^2, \tag{14}$$

where $\mu = mA_1A_2/(A_1 + A_2)$ is the reduced mass, with m as the nucleon mass. The assault frequency or the barrier impinging frequency ν_0 is defined as

$$\nu_0 = \frac{v}{R_0} = \frac{(2E_2/\mu)^{1/2}}{R_0}, \tag{15}$$

where R_0 is the radius of the parent nucleus and $E_2 = \frac{1}{2}\mu v^2$ is the kinetic energy of the proton inside the nucleus. Since both the emitted proton and the daughter nucleus are produced in the ground state, the entire positive Q value is the total kinetic energy ($Q = E_1 + E_2$) available for the decay process, which is shared between the proton and the daughter product, such that for the emitted proton

$$E_2 = \frac{A_1}{A}Q, \tag{16}$$

and $E_1 = Q - E_2$ is the recoil energy of the daughter nucleus.

III. CALCULATIONS AND RESULTS

A. Proton decay of proton emitters

In Fig. 1, a typical scattering potential calculated using Eq. (7) is plotted for a proton emitter ^{105}Sb emitting a proton and leaving ^{104}Sn as a daughter product. The scattering potential, which is narrow and sharp, is studied for the inclusion of angular momentum also. The dotted line in the figure corresponds to the $\ell = 0\,\hbar$ case. The solid line corresponds to $\ell = 2\,\hbar$. The characteristic quantities such as the turning points (R_a, R_b) and the decay Q_p value are marked

TABLE I. The logarithm of half-lives of p decay from different spherical proton emitters. The asterisk symbol ($*$) in the parent nuclei denotes the isomeric state. The experimental Q_p values, half-lives, and ℓ values are taken from Ref. [9]. Our calculated half-lives are compared with the experimental values and with the results of [2–4].

S. No.	Parent	ℓ ($\hbar$)	Q_p (MeV)	$\log_{10} T_{1/2}(s)$				
				Present	Expt.	[2]	[3]	[4]
1	^{105}Sb	2	0.491	2.085	2.049			2.060
2	^{145}Tm	5	1.753	−5.170	−5.409			
3	^{147}Tm	5	1.071	1.095	0.591	0.380	0.415	0.190
4	^{147}Tm*	2	1.139	−3.199	−3.444	−3.569	−3.678	
5	^{150}Lu	5	1.283	−0.859	−1.180	−1.553	−1.509	−1.740
6	^{150}Lu*	2	1.317	−4.556	−4.523			
7	^{151}Lu	5	1.255	−0.573	−0.896	−1.237	−1.222	−1.440
8	^{151}Lu*	2	1.332	−4.715	−4.796			
9	^{155}Ta	5	1.791	−4.637	−4.921			
10	^{156}Ta	2	1.028	−0.461	−0.620	−0.745	−1.013	−0.930
11	^{156}Ta*	5	1.130	1.446	0.949		0.799	
12	^{157}Ta	0	0.947	−0.126	−0.523		−0.658	−1.220
13	^{160}Re	2	1.284	−3.109	−3.046	−3.215	−3.638	−3.480
14	^{161}Re	0	1.214	−3.231	−3.432		−3.721	−3.640
15	^{161}Re*	5	1.338	−0.458	−0.488		−1.066	
16	^{164}Ir	5	1.844	−4.193	−3.959			
17	^{165}Ir*	5	1.733	−3.428	−3.469		−4.000	−4.170
18	^{166}Ir	2	1.168	−1.160	−0.824		−1.678	−0.980
19	^{166}Ir*	5	1.340	0.021	−0.076		−0.553	
20	^{167}Ir	0	1.086	−0.943	−0.959		−1.444	−1.550
21	^{167}Ir*	5	1.261	0.890	0.875		−2.699	
22	^{171}Au	0	1.469	−4.794	−4.770			−3.220
23	^{171}Au*	5	1.718	−2.917	−2.654		−3.456	
24	^{177}Tl	0	1.180	−0.993	−1.174			−5.000
25	^{177}Tl*	5	1.986	−4.379	−3.347			
26	^{185}Bi	0	1.624	−5.184	−4.229		−5.495	−4.890

in the figure. The area under the curve from R_a to R_b is a measure of the probability of penetrating the nuclear interaction barrier.

Figure 2 and Table I depict the comparison of our calculated logarithmic half-lives for different proton emitters with the experimental values. Table I also lists the experimental half-lives and the Q_p values. The ℓ values in Table I are as suggested in the experimental literature. It is to be noted here that in all the experiments performed to date, only the half-life and the energy of the proton are measured. The spin and parity are not experimental observables; such assignments in experimental papers are based on calculated decay rates. The asterisk ($*$) symbol in the parent nuclei denotes the isomeric state. In Fig. 2 the + symbols with a dotted line correspond to our calculated values of the logarithm of half-lives for the ℓ values listed in Table I, and the open squares with a solid line correspond to the experimental values of logarithm of half-lives. In Fig. 2 the calculated logarithms of half-lives are plotted against different proton emitters in the same order as given in Table I (in other words, the value of the x axis corresponds to the S. No. of Table I).

In Table I our calculated results are also compared with the theoretical results of [2–4]. Overall our results are in fair agreement with the experimental values and with other theoretical values. Note that there is no parameter involved in this model. For the proton emitters ^{147}Tm, ^{150}Lu, ^{151}Lu, ^{156}Ta*, ^{157}Ta, ^{177}Tl*, and ^{185}Bi there is clearly a deviation between our calculated values and the experimental values. The discrepancy in these cases may be due to the radius expression (Eq. 6) used in our model or the experimental uncertainties in the measurement of the Q value. Note that in Ref. [2] different radii are chosen to produce a quasi bound state at the Q value. In Ref. [2] the interaction between the odd proton and the remaining core nucleons is described by the Woods-Saxon real part and the related Thomas spin-orbit term, Coulomb potential, and Langer modified centrifugal barrier. In Ref. [3] various theoretical approaches, such as distorted wave born approximation, the two potential approach, and quasiclassical methods, were used to investigate the proton emission from spherical-proton-emitting nuclei using the proton optical potential which was approximated by an average Woods-Saxon field containing the central term and the spin-orbit potential. The depth of the central potential V_0 was adjusted to reproduce the experimental energy of a quasistationary state. Using the effective liquid drop model Guzman *et al*. [4] have calculated the half-lives of various proton emitters. In their work (using the effective liquid drop model) the angular momentum (ℓ) values for the

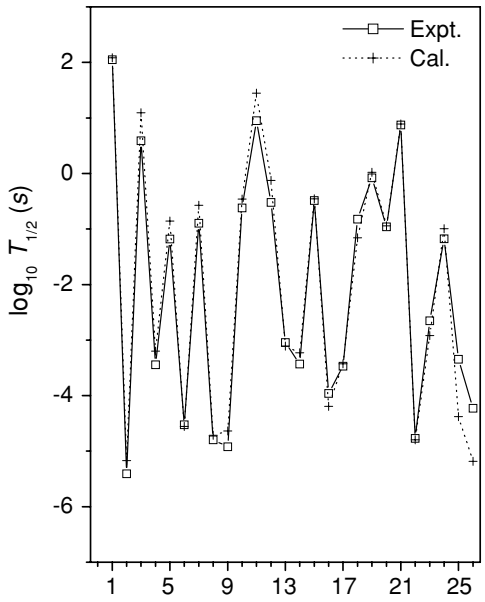

FIG. 2. The logarithm of half-lives for p decay of different proton emitters given in the same order as in Table I (the x-axis numbers correspond to the S. No. in Table I). The + symbols with a dotted line correspond to our calculated values, and the open squares with a solid line correspond to the experimental values.

proton decay of ^{156}Ta, ^{161}Re, and ^{171}Au are chosen in such a way as to give the best agreement between calculated and measured half-life values but are not the ones suggested in the experimental literature. In the present work no attempt is made by means of changing any parameter to find exact agreement between our calculated values and the measured values.

B. α decay of proton emitters

Recently, in some experiments, ground and isomeric proton and alpha decay branches have been reported for ^{177}Tl and ^{185}Bi [1,7]. Also, new ground state α decays for ^{169}Ir and ^{173}Au are reported in [7]. In this study we have investigated the α decay from all the proton emitters in the ground state. The preformation factor P_0 is taken as unity for α-decay calculations also. The angular momentum effects are not included in the present study. The calculations were performed only for s waves ($\ell = 0$ case). The calculated results are presented in Table II. In Table II the Q values for α decay are given in the third column. The Q values are calculated using the experimental mass compilation of Audi and Wapstra [10]. We used the theoretical masses of Möller *et al*. [11] for the cases in which experimental mass is not known. For ^{177}Tl,^{173}Au, and ^{169}Ir the Q values are taken from [7], and the corresponding experimental values for the half-lives are also listed in Table II. For ^{157}Ta the experimental half-life is taken from [12]. Using the generalized liquid drop model (GLDM) [12] for ^{157}Ta the logarithm of half-life is calculated as -2.52. Our calculated values are in fair agreement with the available experimental values. Hence the important outcome of the present work is that half-lives of α decay from all the observed proton emitters from the ground state are well within the experimentally measurable limits. Hence α-decay branching can be a competing mode for all the observed proton emitters from the ground state.

TABLE II. The logarithm of half-lives of α decay from different proton emitters. The Q values are calculated from [10,11].

S. No.	Parent	Q value	$\log_{10} T_{1/2}^{\text{cal.}}(s)$	$\log_{10} T_{1/2}^{\text{exp.}}(s)$
1	^{105}Sb	2.203	11.082	
2	^{109}I	3.782	−0.639	
3	^{112}Cs	4.133	−1.393	
4	^{113}Cs	3.484	2.392	
5	^{117}La	2.675	10.505	
6	^{131}Eu	3.555	6.818	
7	^{140}Ho	4.165	4.978	
8	^{141}Ho	4.095	5.401	
9	^{145}Tm	4.225	5.696	
10	^{146}Tm	3.755	8.935	
11	^{147}Tm	3.528	10.721	
12	^{150}Lu	3.325	13.844	
13	^{151}Lu	3.226	14.778	
14	^{155}Ta	3.045	18.058	
15	^{156}Ta	5.101	2.776	
16	^{157}Ta	6.382	−2.662	−2.28
17	^{160}Re	6.699	−2.938	
18	^{161}Re	6.439	−2.048	
19	^{164}Ir	6.895	−2.811	
20	^{165}Ir	6.815	−2.564	
21	^{166}Ir	6.703	−2.198	
22	^{167}Ir	6.495	−1.476	
23	^{169}Ir	6.005	0.390	−0.195
24	^{171}Au	7.106	−2.799	
25	^{173}Au	6.672	−1.350	−1.710
26	^{177}Tl	6.907	−1.390	−1.745
27	^{185}Bi	7.639	−3.123	

IV. SUMMARY

In this paper, we have studied the proton and α decay of all the observed proton emitters using a unified fission model modified from the preformed cluster model of Gupta and collaborators. Our calculated results for proton decay half-lives compare fairly well with the experimental values. The discrepancy between our results and the experimental values for some cases may be due to the radius expression used in the model or the uncertainty in the measurement of the Q_p value. We have applied the same model to study the α decay of all the proton emitters for s waves. We find that α-decay branching can be a competing mode for all the observed proton emitters.

ACKNOWLEDGMENTS

One of the authors (M.B.) acknowledges with thanks the partial financial support of the Department of Science and Technology (DST), vide Grant No. SR/FTP/PSA-02/2002.

Also, the support by DST under the FIST programme vide letter No. SR/FST/PSI-005/2000 to the Department of Physics, M.S. University, Tirunelveli, India, is gratefully acknowledged.

[1] G. L. Poli *et al*., Phys. Rev. C **63**, 044304 (2001).
[2] B. Buck, A. C. Merchant, and S. M. Perez, Phys. Rev. C **45**, 1688 (1992).
[3] S. Aberg, P. B. Semmes, and W. Nazarewicz, Phys. Rev. C **56**, 1762 (1997).
[4] F. Guzman *et al*., Phys. Rev. C **59**, R2339 (1999).
[5] S. S. Malik and R. K. Gupta, Phys. Rev. C **39**, 1992 (1989).
[6] M. Balasubramaniam and R. K. Gupta, Phys. Rev. C **60**, 064316 (1999).
[7] G. L. Poli *et al*., Phys. Rev. C **59**, R2979 (1999).
[8] J. Blocki, J. Randrup, W. J. Swiatecki, and C. F. Tsang, Ann. Phys. (NY) **105**, 427 (1977).
[9] A. A. Sonzogni, Nuclear Data Sheets **95**, 1 (2002).
[10] G. Audi and A. H. Wapstra, Nucl. Phys. **A595**, 409 (1995).
[11] P. Möller, J. R. Nix, W. D. Myers, and W. J. Swiatecki, At. Data Nucl. Data Tables **59**, 185 (1995).
[12] G. Royer, J. Phys. G **26**, 1149 (2000).